Available online at www.sciencedirect.com
ScienceDirect
Journal of Sound and Vibration 319 (2009) 392–405
JOURNAL OF SOUND AND VIBRATION
www.elsevier.com/locate/jsvi

Thermoelastic damping of the axisymmetric vibration of circular plate resonators

Yuxin Sun*, Hironori Tohmyoh

Department of Nanomechanics, Tohoku University, Aoba 6-6-01, Aramaki, Aoba-ku, Sendai 980-8579, Japan

Received 12 December 2007; received in revised form 17 May 2008; accepted 4 June 2008
Handling Editor: L.G. Tham
Available online 24 July 2008

Abstract

Thermoelastic damping is recognized as a significant loss mechanism at room temperature in micro-scale circular plate resonators. In this paper, the governing equations of coupled thermoelastic problems are established for axisymmetric out-of-plane vibration of circular plate. Then the analytical expression for thermoelastic damping is obtained. The effects of environmental temperature, plate dimensions and boundary conditions on the thermoelastic damping are studied.

1. Introduction

Micro-scale mechanical resonators have high sensitivity as well as fast response [1–3] and are widely used as sensors and modulators [4–6]. It is necessary to know how the parameters affect their physical and mechanical behaviours. For resonators, it is desired to design and construct systems with loss of mechanical energy as little as possible. Unfortunately, it has been consistently observed that there exists energy dissipation that increases with size decreasing significantly—even when made from pure single-crystal materials [7]. Many researchers have discussed different dissipation mechanisms in MEMS [8–14], such as doping-impurities losses, support-related losses, thermoelastic damping and the Akhiezer effect [8], as well as the radiation of energy away from the resonator into its surroundings. Mihailovich and MacDonald [9] measured the mechanical loss of various micron-sized vacuum-operated single-crystal silicon resonators, to identify their dominant loss mechanism. They examined three possible sources of mechanical loss, including doping-impurity losses, support-related losses and surface-related losses. Zhang et al. [10] studied the effect of air damping on the frequency response and the quality factor of a micro-machined beam resonator. Their results indicate that air damping generally shifts the resonance frequency on the order of no more than 10^{-6} and degrades the quality factor, and that this effect of air damping increases as the dimension of the beam decreases. Harrington et al. [11] measured mechanical dissipation in micron-sized single-crystal gallium arsenide resonators that vibrate in torsion and flexural modes. They found that the resonance frequency changes with temperature.

*Corresponding author. Tel.: +81 227956898.
E-mail address: sunyx@ism.mech.tohoku.ac.jp (Y. Sun).

0022-460X/$ - see front matter © 2008 Elsevier Ltd. All rights reserved.
doi:10.1016/j.jsv.2008.06.017

It has been verified that thermoelastic damping is a significant loss mechanism near room temperature in MEMS resonators [15]. Zener [16,17] predicted the existence of the thermoelastic damping process and then quickly verified the basic aspects of the theory experimentally [18]. Further experiments consistent with Zener's theory were provided by Berry [19] for α-brass, in which case the damping was measured as a function of frequency at room temperature. Roszhart [20] observed thermoelastic damping in single-crystal silicon micro-resonators at room temperature. Yasumura et al. [21] also reported thermoelastic damping in silicon nitride micro-resonators at room temperature, and their measured results are an order of magnitude smaller than Roszhart's. Houston et al. [22] studied the importance of thermoelastic damping for silicon-based MEMS. Their results indicate that the internal friction arising from this mechanism is strong and persists down to 50 nm scale structures. Lifshitz and Roukes [7] studied thermoelastic damping of a beam with rectangular cross-sections, and found that after the Debye peaks, the thermoelastic attenuation will be weakened as the size increases. Srikar and Senturia [23] studied thermoelastic damping in fine-grained polysilicon flexural beam resonators, and found that single-crystal silicon, rather than fine-grained polysilicon, is the material of choice for the fabrication of flexural beam resonators for applications in the gigahertz frequency range.

This paper deals with thermoelastic damping effects on the out-of-plane vibration of circular plate resonators. Circular plates are common elements in many sensors and resonators [24]. For example, Vig et al. [25] proposed a micro-resonator-based high sensitivity sensor and sensor array for use as infrared (IR) sensors. Micro-scale circular resonators may have thickness of 1–10 μm and diameter of 10^2–10^3 μm, with resonance frequencies of the fundamental mode (thickness shear mode) in the range of 100–1000 MHz. Although such micro-resonators are not suitable for precision frequency control applications due to their extremely high sensitivity to mass loading, they can be used for IR detection and imaging, and for chemical and biological agent sensing. In particular, when quartz is used as the resonator material, the temperature dependence of the resonance frequency can be utilized to make precision thermometers [26,27].

Such resonators can be considered as a thin circular plate. So the governing equation of the thermoelastic coupling problem for this resonator can be derived through thin plate theory in cylindrical coordinates. This paper will give a simple derivation of the approximate thermoelastic equations for a thin circular plate under out-of-plane vibration and then solve these equations to arrive at an exact expression for thermoelastic damping in circular plates.

2. Process of thermoelastic damping

An elastic wave dissipates energy due to intrinsic and extrinsic mechanisms. Some of the extrinsic mechanisms are affected by changes of environment; for example, air damping can be minimized under ultrahigh-vacuum conditions. The intrinsic dissipation mechanism can be regarded as phonon–phonon interaction, namely the scattering of acoustic phonons with thermal phonons [7].

When an elastic solid is set in motion, it is taken out of equilibrium, having an excess of kinetic and potential energy. The coupling of the strain field to a temperature field provides an energy dissipation mechanism that allows the system to relax back to equilibrium. This process of energy dissipation, called thermoelastic damping, is what we will discuss in this paper.

Zener [16,17] firstly developed the thermoelastic damping theory by studying the transverse vibration of homogeneous and isotropic thin beam. Thermoelastic damping arises from thermal currents generated by compression tension in elastic media. The bending of the reed causes dilations of opposite signs to exist on the upper and lower halves. One side is compressed and heated, and the other side is stretched and cooled. Thus, in the presence of finite thermal expansion, a transverse temperature gradient is produced. The temperature gradient generates local heat currents, which cause increase of the entropy of the reed and lead to energy dissipation. The temperature across the reed equalizes in a characteristic time τ_R, while the vibration frequency of the reed is ω. In the low-frequency range, i.e., $\tau_R \ll \omega^{-1}$, the vibrations are isothermal and a small amount of energy is dissipated. On the other hand, for $\tau_R \gg \omega^{-1}$, adiabatic conditions prevail with low-energy dissipation similar to the low-frequency range. While $\tau_R \approx \omega^{-1}$, stress and strain are out of phase and a maximum of internal friction occurs. This is the so-called Debye peak.

For a beam of thickness h, with a rectangular cross-section, its characteristic time is

$$\tau_R = (h/\pi)^2 \chi^{-1}, \tag{1}$$

where $\chi = \kappa/\rho c_v$ is the thermal diffusion coefficient, in which ρ, κ and c_v are the density, thermal conductivity and specific heat at constant volume, respectively. The vibration frequency of a beam is

$$\omega = \frac{q^2 h}{L^2}\sqrt{\frac{E}{12\rho}}, \tag{2}$$

where E is Young's modulus, L the beam length and the allowed values of q are determined by the supporting conditions at the two ends of the beam.

In Zener's theory [16,17], the classical Fourier thermal conduction theory is applied and there is no heat flow perpendicular to the surfaces of the beam. Thus, the internal friction, Q^{-1} (Q is the quality factor defined by Zener), is defined as follows:

$$Q^{-1} = \frac{\alpha_T^2 TE}{C_p}\frac{\omega\tau_R}{1+\omega^2\tau_R^2}, \tag{3}$$

where C_p is the specific heat at constant pressure, α_T the coefficient of linear thermal expansion, T the temperature of the reed and ω and τ_R are defined in Eqs. (1) and (2).

Lifshitz and Roukes [7] gave another expression for the thermoelastic damping by

$$Q^{-1} = \frac{\alpha_T^2 TE}{C_p}\left(\frac{6}{\xi^2} - \frac{6}{\xi^3}\frac{\sinh\,\xi + \sin\,\xi}{\cosh\,\xi + \cos\,\xi}\right), \tag{4}$$

in which $\xi = h\sqrt{\omega/2D}$.

Wong et al. [28] considered thermoelastic damping of the in-plane vibration of thin silicon rings of rectangular cross-section. Analysis of thermoelastic damping developed by Zener and by Lifshitz and Roukes was extended to cover the in-plane flexural vibration of thin rings. The expression of Q^{-1} for the ring obtained by Wong et al. is the same as that for a beam obtained by Zener and by Lifshitz and Roukes except that the characteristic length varies according to the shape of the resonators. For a wide range of ring size relevant to MEMS resonators, the values of Q-factor predicted by the two approaches agree to within ~2% for low-order flexural modes.

This paper studies the thermoelastic damping effect on the vibration of circular plate. Section 3 gives the derivation of the thermoelastic equations for a circular plate under out-of-plane flexural vibration. Section 4 solves these equations and arrives at an exact expression for thermoelastic damping in circular plate. In Section 5, the validity of Zener's theory on analyzing the thermoelastic damping in circular plate is verified, and the effects of plate size, boundary conditions and environmental temperature on the thermoelastic damping are analyzed for silicon plate.

3. Formulation of basic equations

This section will derive the governing equations for the thermoelastic coupling problem of circular plate vibration. To simplify the derivation for thin circular plates, the following basic hypotheses, including the Kirchhoff–Love plate theory, are employed in the analysis [29]:

(a) Normal stress σ_{zz} can be neglected relative to the principal stresses, i.e., $\sigma_{zz} = 0$.
(b) The rectilinear element normal to the middle surface before deformation remains perpendicular to the strained surface after deformation and their elongation can be neglected, i.e., $\varepsilon_{rz} = \varepsilon_{\theta z} = 0$.
(c) For small deformation vibration, the deformation along the middle surface can be neglected, i.e., $\varepsilon_{zz} = 0$.

3.1. Equation of transverse motion for a thin circular plate

Consider a thin circular plate with uniform thickness h and radius a, as is shown in Fig. 1(a). The cylindrical coordinate system (r, θ, z) is applied to study the vibration of the circular plate, with an origin located at the

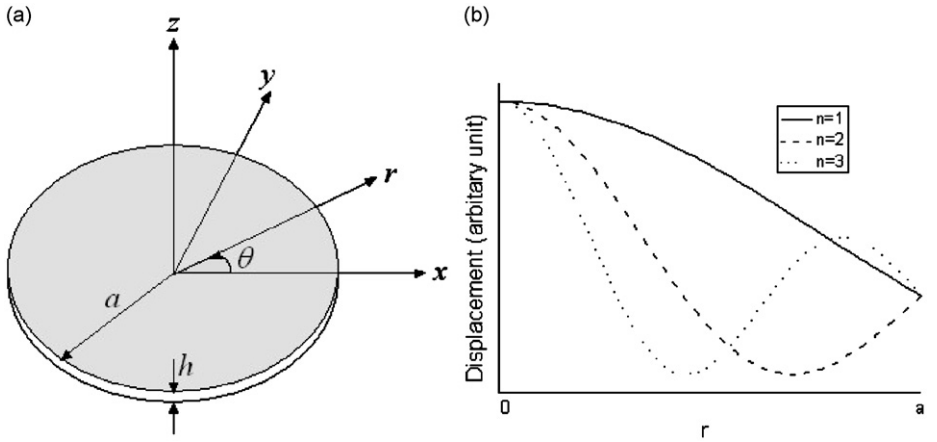

Fig. 1. (a) Schematic illustration of the circular plate and the coordinate system, (b) the first three mode shapes of a simply supported circular plate along the r-direction.

center of the plate. We put the neutral surface on the (r, θ) coordinate plane, and the z-axis normal to the neutral surface. The circular plate is made of silicon. In equilibrium, the plate is unstrained, unstressed and keeps at environmental temperature T_0 everywhere.

Circular plates are capable of both in-plane and out-of-plane vibrations, but only out-of-plane vibrations are considered in this paper. We define $u(r, \theta, z, t)$, $v(r, \theta, z, t)$ and $w(r, \theta, z, t)$ to be the displacement components along the radial, circumferential and axial directions, respectively, and $T(r, \theta, z, t)$ the temperature field. According to the above hypotheses, the relationship between the displacements can be given by

$$\begin{aligned} u(r,\theta,z,t) &= -z\frac{\partial w(r,\theta,t)}{\partial r},\\ v(r,\theta,z,t) &= -z\frac{\partial w(r,\theta,t)}{r\partial\theta},\\ w(r,\theta,z,t) &= w(r,\theta,t), \end{aligned} \tag{5}$$

where t is the time.

The strain components are given by

$$\begin{aligned} \varepsilon_r &= \frac{\partial u}{\partial r} = -z\frac{\partial^2 w}{\partial r^2},\\ \varepsilon_\theta &= \frac{u}{r} + \frac{\partial v}{r\partial\theta} = -z\left(\frac{\partial w}{r\partial r} + \frac{\partial^2 w}{r^2\partial\theta^2}\right),\\ \gamma_{r\theta} &= \frac{\partial u}{r\partial\theta} + \frac{\partial v}{\partial r} - \frac{v}{r} = -2z\frac{\partial}{\partial r}\left(\frac{\partial w}{r\partial\theta}\right). \end{aligned} \tag{6}$$

The cubical dilatation e is thus obtained as

$$e = \varepsilon_r + \varepsilon_\theta = -z\nabla^2 w. \tag{7}$$

Stress components are given by the constitutive equation as

$$\begin{aligned} \sigma_r &= \frac{E}{1-v^2}[(\varepsilon_r + v\varepsilon_\theta) - (1+v)\alpha_T\vartheta] = -\frac{E}{1-v^2}\left[z\frac{\partial^2 w}{\partial r^2} + vz\left(\frac{\partial w}{r\partial r} + \frac{\partial^2 w}{r^2\partial\theta^2}\right) + (1+v)\alpha_T\vartheta\right],\\ \sigma_\theta &= \frac{E}{1-v^2}[(\varepsilon_\theta + v\varepsilon_r) - (1+v)\alpha_T\vartheta] = -\frac{E}{1-v^2}\left[z\left(\frac{\partial w}{r\partial r} + \frac{\partial^2 w}{r^2\partial\theta^2}\right) + vz\frac{\partial^2 w}{\partial r^2} + (1+v)\alpha_T\vartheta\right],\\ \tau_{r\theta} &= G\varepsilon_{r\theta} = -2Gz\frac{\partial}{\partial r}\left(\frac{\partial w}{r\partial\theta}\right), \end{aligned} \tag{8}$$

where G is the shear modulus and $\vartheta = T - T_0$ the temperature increment of the resonator as a function of (r, θ, z, t).

Thus, we can get the moments of flexure and torsion as follows:

$$M_r = \int_{-h/2}^{h/2} \sigma_r z \, dz = -D\left[\frac{\partial^2 w}{\partial r^2} + v\left(\frac{\partial w}{r\partial r} + \frac{\partial^2 w}{r^2 \partial \theta^2}\right) + (1+v)\alpha_T M_T\right],$$
$$M_\theta = \int_{-h/2}^{h/2} \sigma_\theta z \, dz = -D\left[\left(\frac{\partial w}{r\partial r} + \frac{\partial^2 w}{r^2 \partial \theta^2}\right) + v\frac{\partial^2 w}{\partial r^2} + (1+v)\alpha_T M_T\right],$$
$$M_{r\theta} = \int_{-h/2}^{h/2} \tau_{r\theta} z \, dz = -D(1-v)\frac{\partial}{\partial r}\left(\frac{\partial w}{r\partial \theta}\right), \tag{9}$$

where

$$M_T = \frac{12}{h^3}\int_{-h/2}^{h/2} \vartheta z \, dz$$

is the thermal moment, and

$$D = \frac{Eh^3}{12(1-v^2)}.$$

The equation of transverse motion for a circular plate is

$$\frac{\partial^2 M_r}{\partial r^2} + \frac{\partial}{\partial r}\left(\frac{\partial M_{r\theta}}{r\partial \theta}\right) + \frac{\partial}{r\partial \theta}\left(\frac{\partial M_{r\theta}}{\partial r}\right) + \frac{\partial}{r\partial \theta}\left(\frac{\partial M_\theta}{r\partial \theta}\right) - \rho h \frac{\partial^2 w}{\partial t^2} = 0. \tag{10}$$

Substituting Eq. (9) into Eq. (10) yields the differential equation of the lateral vibration of the plate

$$D\nabla^2\nabla^2 w + D(1+v)\alpha_T \nabla^2 M_T + \rho h \frac{\partial^2 w}{\partial t^2} = 0, \tag{11}$$

where ρ is the density of the plate and ∇^2 the Laplace operator in the polar coordinate system. For axisymmetric circular plate, the displacement and thermal moment are independent of θ, so the Laplace operator is

$$\nabla^2 = \frac{\partial^2}{\partial r^2} + \frac{1}{r}\frac{\partial}{\partial r}. \tag{12}$$

3.2. Thermal conduction equation for circular plate

The thermal conduction equation containing the thermoelastic coupling term has the following form:

$$\kappa\nabla^2\vartheta + \kappa\frac{\partial^2 \vartheta}{\partial z^2} = \rho c_v \frac{\partial \vartheta}{\partial t} + \beta T_0 \frac{\partial e}{\partial t}, \tag{13}$$

where c_v is the specific heat at constant volume, κ the thermal conductivity and $\beta = E\alpha_T/(1-2v)$ the thermal modulus, in which α_T is the coefficient of thermal expansion and v the Poisson's ratio.

Substituting Eq. (7) into Eq. (13) gives the thermal conduction equation for the plate

$$\kappa\nabla^2\vartheta + \kappa\frac{\partial^2 \vartheta}{\partial z^2} = \rho c_v \frac{\partial \vartheta}{\partial t} - \beta T_0 z \frac{\partial}{\partial t}(\nabla^2 w). \tag{14}$$

This paper only considers the axisymmetric problem for a circular plate. Noting that thermal gradients in the plane of the cross-section along the plate thickness direction are much larger than gradients along the radial direction, we can ignore the term $\nabla^2\vartheta$ in the thermal conduction equation. In summary, we can get the

governing equation of this problem as

$$D\nabla^2\nabla^2 w + D(1+v)\alpha_T\nabla^2 M_T + \rho h\frac{\partial^2 w}{\partial t^2} = 0, \tag{15}$$

$$\kappa\frac{\partial^2 \vartheta}{\partial z^2} = \rho c_v\frac{\partial \vartheta}{\partial t} - \beta T_0 z\frac{\partial}{\partial t}(\nabla^2 w). \tag{16}$$

4. Thermoelastic damping in a circular plate

4.1. Solution of the thermoelastic equations

To calculate the effect of thermoelastic coupling on the vibrations of a circular plate, we solve the coupled thermoelastic Eqs. (15) and (16) for the case of harmonic vibrations. We set

$$w(r,t) = w_0(r)\mathrm{e}^{\mathrm{i}\omega t}, \quad \vartheta(r,z,t) = \vartheta_0(r,z)\mathrm{e}^{\mathrm{i}\omega t}, \tag{17}$$

where ω is the frequency and $w_0(r)$ the mode shape. We expect to find that in general the frequency ω is complex, the real part $\mathrm{Re}(\omega)$ giving the new eigenfrequencies of the plate in the presence of thermoelastic coupling effect, and the imaginary part $|\mathrm{Im}(\omega)|$ giving the attenuation of the vibration.

Substituting Eq. (17) into Eqs. (15) and (16) yields the following equations:

$$D\nabla^2\nabla^2 w_0 + D(1+v)\alpha_T\nabla^2 M_{T0} - \rho h\omega^2 w_0 = 0, \tag{18}$$

$$\kappa\frac{\partial^2 \vartheta_0}{\partial z^2} = \mathrm{i}\omega\rho c_v\vartheta_0 - \mathrm{i}\omega\beta T_0 z\nabla^2 w_0, \tag{19}$$

where

$$M_{T0} = \frac{12}{h^3}\int_{-h/2}^{h/2}\vartheta_0 z\,\mathrm{d}z. \tag{20}$$

The solution of Eq. (19) is

$$\vartheta_0 - \frac{\beta T_0}{\rho c_v}z\nabla^2 w_0 = A\,\sin(mz) + B\,\cos(mz), \tag{21}$$

where

$$m = \sqrt{-\frac{\mathrm{i}\omega\rho c_v}{\kappa}} = (1-\mathrm{i})\sqrt{\frac{\omega\rho c_v}{2\kappa}}, \tag{22}$$

where i is the square root of -1.

There is no flow of heat across the upper and lower surfaces of the plate so that $\partial\vartheta_0/\partial z = 0$ at $z = \pm h/2$. Thus, the coefficients A and B are determined as

$$A = -\frac{\beta T_0}{\rho c_v}\frac{1}{m\,\cos(mh/2)}\nabla^2 w_0,$$
$$B = 0. \tag{23}$$

The temperature profile $\vartheta_0(r, z)$ across the plate is then given by

$$\vartheta_0(r,z) = \frac{\beta T_0}{\rho c_v}\nabla^2 w_0\left(z - \frac{\sin(mz)}{m\,\cos(mh/2)}\right). \tag{24}$$

According to Eqs. (20) and (24), the expression of M_{T0} is obtained as

$$M_{T0} = \Delta_M(1+f(\omega))\nabla^2 w_0, \tag{25}$$

where

$$\Delta_M = \frac{\beta T_0}{\rho c_v}, \quad f(\omega) = \frac{24}{m^3 h^3}\left(\frac{mh}{2} - \tan\left(\frac{mh}{2}\right)\right). \tag{26}$$

Substitution of Eq. (25) into Eq. (18) gives

$$D_\omega \nabla^2 \nabla^2 w_0 - \rho h \omega^2 w_0 = 0, \tag{27}$$

where

$$D_\omega = D(1 + \Delta_D(1 + f(\omega))), \tag{28}$$

$$\Delta_D = (1+v)\alpha_T \Delta_M = \frac{(1+v)\alpha_T \beta T_0}{\rho c_v}. \tag{29}$$

For axisymmetric vibration of circular plate, the solution of Eq. (27) is

$$w_0(r) = A_0 J_0(pr) + B_0 Y_0(pr) + C_0 I_0(pr) + D_0 K_0(pr), \tag{30}$$

where $p^4 = \rho h \omega^2 / D_\omega$, and the coefficients A_0 through D_0 and the allowed values of p are determined by the boundary conditions. Due to the limitation of $w_0(r)$ at the plate center ($r = 0$), we get $B_0 = D_0 = 0$, that is

$$w_0(r) = A_0 J_0(pr) + C_0 I_0(pr). \tag{31}$$

In this paper, two kinds of boundary conditions are considered. On the one hand, boundary conditions regarding movements in the case of a clamped plate have the form of

$$\begin{cases} w_0|_{r=a} = 0, \\ \left.\dfrac{\mathrm{d}w_0}{\mathrm{d}r}\right|_{r=a} = 0. \end{cases} \tag{32}$$

Substitute expression of deflection, i.e., Eq. (31), into the boundary conditions, i.e., Eq. (32), we have

$$\begin{cases} A_0 J_0(pa) + C_0 I_0(pa) = 0, \\ -A_0 p J_1(pa) + C_0 p I_1(pa) = 0. \end{cases} \tag{33}$$

In order to get nontrivial solutions, the constants A_0 and C_0 must be nonzero. Therefore, we obtain the following frequency equation:

$$\begin{vmatrix} J_0(pa) & I_0(pa) \\ -J_1(pa) & I_1(pa) \end{vmatrix} = 0. \tag{34}$$

The allowed value of pa may be obtained through solving Eq. (34) as $pa = \sqrt{q_n}$, where $q_n = \{10.21, 39.78, 89.10, \ldots\}$.

On the other hand, in the case of a simply supported plate, the boundary conditions become

$$\begin{cases} w_0|_{r=a} = 0, \\ [\nabla^2 w_0 + (1+v)\alpha_T M_{T0}]|_{r=a} = 0. \end{cases} \tag{35}$$

According to Eq. (25), the second expression in Eq. (35) can be changed to

$$\{[1 + (1+v)\alpha_T \Delta_M (1 + f(\omega))]\nabla^2 w_0\}|_{r=a} = 0, \tag{36}$$

namely,

$$\nabla^2 w_0|_{r=a} = 0. \tag{37}$$

So the boundary conditions for a simply supported plate has the following form:

$$\begin{cases} w_0|_{r=a} = 0, \\ \nabla^2 w_0|_{r=a} = 0. \end{cases} \tag{38}$$

Substituting Eq. (31) into Eq. (38) yields the following frequency equation:

$$\begin{vmatrix} J_0(\mathrm{pa}) & I_0(\mathrm{pa}) \\ J_0(\mathrm{pa}) & -I_0(\mathrm{pa}) \end{vmatrix} = 0, \tag{39}$$

whose solution is $\mathrm{pa} = \sqrt{q_n}$, where $q_n = \{4.977, 29.76, 74.20, \ldots\}$.

From Eqs. (31), (34) and (39), we can obtain the mode shape of the clamped and the simply supported plate, respectively. To make the problem intuitionistic, in Fig. 1(b), we present the first three mode shapes of a simply supported circular plate along the r-direction.

Now the vibration frequency of the circular plate considering thermoelastic coupling effect can be drawn from the expression of $p^4 = \rho h\omega^2/D_\omega$, namely,

$$\omega = p^2\sqrt{\frac{D_\omega}{\rho h}} = \omega_0\sqrt{1 + \Delta_D(1 + f(\omega))}, \tag{40}$$

where ω_0 is the eigenfrequency when thermoelastic coupling effect is ignored with the expression of

$$\omega_0 = \frac{q_n}{a^2}\sqrt{\frac{D}{\rho h}}. \tag{41}$$

Noting that $\Delta_D \ll 1$ for silicon ($\Delta_D = 1.26 \times 10^{-4}$ for $T_0 = 293\,\mathrm{K}$), we can replace $f(\omega)$ in the square root by $f(\omega_0)$ and expand Eq. (40) into a series up to first order. Then Eq. (40) becomes

$$\omega = \omega_0\left[1 + \frac{\Delta_D}{2}(1 + f(\omega_0))\right]. \tag{42}$$

By the convenient substitution

$$\xi = h\sqrt{\frac{\omega_0\rho c_v}{2\kappa}}, \tag{43}$$

we can easily extract the real and imaginary parts, giving the vibration frequency of the plate together with the corresponding attenuation coefficient [7],

$$\mathrm{Re}(\omega) = \omega_0\left[1 + \frac{\Delta_D}{2}\left(1 - \frac{6}{\xi^3}\frac{\sinh\xi - \sin\xi}{\cosh\xi + \cos\xi}\right)\right], \tag{44}$$

$$\mathrm{Im}(\omega) = \omega_0\frac{\Delta_D}{2}\left(\frac{6}{\xi^3}\frac{\sinh\xi + \sin\xi}{\cosh\xi + \cos\xi} - \frac{6}{\xi^2}\right). \tag{45}$$

Thus, we arrive at an expression for thermoelastic damping in a circular plate, which is given by

$$Q^{-1} = 2\left|\frac{\mathrm{Im}(\omega)}{\mathrm{Re}(\omega)}\right| = \Delta_D\left(\frac{6}{\xi^2} - \frac{6}{\xi^3}\frac{\sinh\xi + \sin\xi}{\cosh\xi + \cos\xi}\right). \tag{46}$$

It can be seen that Eq. (46) has the similar form to Eq. (4).

4.2. Concise analysis based on Zener's approach

It is shown in Eq. (6) that the radial strain in the plate is directly proportional to z, the axial distance from the neutral plane. According to Zener's approach, the quality τ_R is the relaxation time for the establishment of temperature equilibrium across the thickness of beam. Effectively, the relaxation time τ_R has the same meaning in the circular plate as in a thin beam [28]. Alternating temperature gradient exists between the upper and lower surfaces of the plate during vibration. As a result, unidirectional heat flow and relaxation across the thickness of the plate causes energy to be dissipated. Thus, it can be argued that thermoelastic damping in plates undergoing out-of-plane flexural vibrations can be modeled using Zener's approach as developed for slender beam, Eqs. (1) and (3). On this basis, the Q^{-1}-factor of a circular plate is given by Eq. (3) using

a relaxation time based on the thickness of the plate, i.e.,

$$\tau_R = \left(\frac{h}{\pi}\right)^2 \frac{\rho c_v}{\kappa}, \tag{47}$$

and the natural frequency of the plate is given by Eq. (41).

5. Results and discussions

In this section, the relationship between Q^{-1}, plate dimensions, boundary conditions and vibration modes for silicon MEMS devices under different environmental temperatures are explored. According to the theory outlined in Section 4, it is possible to predict thermoelastic damping for silicon plate as a function of radius a, thickness h, and mode number n.

We use the literature values of the thermodynamic properties of silicon for three representative temperatures: 120, 200 and 293 K, where the temperature dependency of E, κ, c_v and α_T was reported as summarized in Table 1 [30]. Noting that, in the range of the temperature considered, temperature dependency of thermal properties of silicon, i.e., κ, c_v and α_T are obvious.

In general, the elastic and thermal properties of silicon are temperature dependent. However, the temperature change associated with thermoelastic vibration is known to be small ($\ll 1$ K) [28] and it is therefore reasonable to treat the mechanical and thermal parameters as constants with values applicable to the environmental temperature T_0. In the following subsections, the $n = 1$ mode will first be considered in detail before considering higher-order modes.

5.1. Thermoelastic damping for plate of $a/h = 50$ under $T_0 = 293$ K

First we consider the case of a circular plate with fixed aspect ratio of $a/h = 50$ under the temperature of $T_0 = 293$ K. When h is varied, a changes accordingly with h. Fig. 2 shows the thermoelastic damping of the

Table 1
Mechanical and thermal properties of silicon under different temperatures

T_0 (K)	E (GPa)	ρ (kg m^{-3})	v	κ (W m^{-1} K^{-1})	c_v (J kg^{-1} K^{-1})	α_T (10^{-6} K^{-1})
120	169.0	2330	0.22	876	328	−0.057
200	166.9	2330	0.22	266	557	1.406
293	165.9	2330	0.22	156	713	2.59

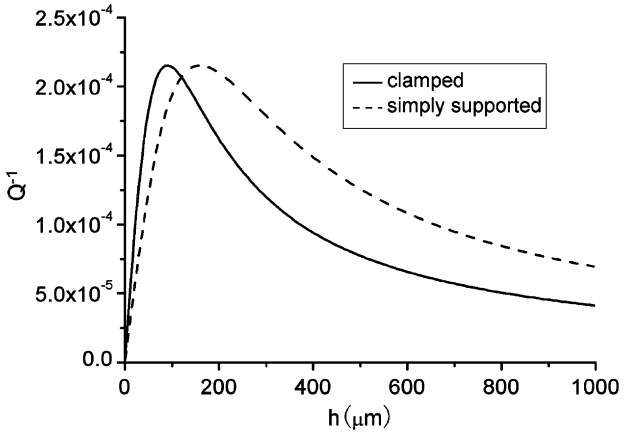

Fig. 2. Variation of thermoelastic damping of a circular plate with thickness. The aspect ratio of the plate is fixed as $a/h = 50$ and the environmental temperature is $T_0 = 293$ K.

circular plate against thickness h. The solid lines present the values for a clamped plate and the dashed lines for a simply supported plate.

It is shown that as the thickness increases, the thermoelastic damping increases first and then decreases, and there is a critical thickness, denoted as h_c, with the maximum value of thermoelastic damping. The maximum value of Q^{-1} are almost the same for both the clamped plate and the simply supported plate. However, the critical thickness for the clamped plate is smaller than that for the simply supported plate.

5.2. Thermoelastic damping for different geometries and boundary conditions

We plot the dependence of thermoelastic damping on geometry in three different ways: (1) Q^{-1} against thickness h for fixed aspect ratio a/h, (2) Q^{-1} against thickness h for fixed radius a and (3) Q^{-1} against radius a for fixed thickness h. The dependence of thermoelastic damping on boundary conditions is also considered. The circular plate is clamped and simply supported, respectively. The outcome is shown in Fig. 3 for the case of a plate vibrating in its fundamental mode ($q_n = 10.21$ for clamped and $q_n = 5.783$ for simply supported plate).

Fig. 3 shows that thermoelastic damping Q^{-1} clearly depends on the geometry of the plate. In addition, the boundary conditions and environmental temperatures also influence the value of Q^{-1}.

First of all, it is shown that under the environmental temperature of $T_0 = 120\,\mathrm{K}$, the thermoelastic damping Q^{-1} is very small. In Gysin's research [31], he tested the internal friction Q^{-1} of the first eigenmode of micro-fabricated silicon cantilevers in the temperature range of 15–300 K and found that the thermoelastic damping depends on temperature clearly and that thermoelastic damping is the smallest under the temperature of 20 and 125 K. Now our calculation also demonstrates this phenomenon.

In addition, as the plate size increases, the thermoelastic damping Q^{-1} first increases and then decreases. And there exits a critical size at which Q^{-1} takes the maximum value. When the plate size is larger than the critical size, Q^{-1} of simply supported plate is larger than that of clamped plate under the same plate size.

Finally, the maximum value of Q^{-1} is independent of the dimensions of the plate and the boundary conditions, but mainly depends on the environmental temperature. It is shown in Fig. 3 that under the same environmental temperature, $Q^{-1}_{\max}$, the maximum value of Q^{-1}, has the same value under the three cases: fixed aspect ratio a/h, fixed plate thickness h, and fixed plate radius a. Furthermore, the value of $Q^{-1}_{\max}$ of clamped plate is the same as that of simply supported plate. These phenomena are due to the temperature dependency of E, α_T and c_v. According to the expression of Q^{-1}, i.e., Eq. (45), we can get $Q^{-1}_{\max} = 0.494\Delta_D$, where Δ_D is a temperature-dependent parameter. It is obvious from Zener's theory that the maximum value of Q^{-1} is independent of dimensions of a beam, as expressed by Eq. (3). Here, we can demonstrate that this phenomenon is also valid for a circular plate.

5.3. Comparison between the present method and Zener's approach

The above analyses show that the thermoelastic damping is size dependent and there is a critical thickness at which the thermoelastic damping reaches maximum value for a plate with fixed aspect ratio of a/h. For the method presented in this paper, the critical thickness can be obtained through the expression of $\mathrm{d}Q^{-1}/\mathrm{d}h = 0$. And for Zener's approach, it is obtained through $\tau_R = \omega_0^{-1}$.

Table 2 presents the critical thicknesses (μm) predicted using the present method and Zener's approach for $a/h = 50$ under different temperatures. It also shows the percentage difference between the two methods, using Zener's approach as the baseline.

It is shown that the values predicted using the present method are a little larger than those by Zener's approach, but the percentage difference between the two methods are quite small under all the conditions of different boundary conditions and environmental temperatures when the aspect ratio is fixed as $a/h = 50$. This demonstrate that the Zener's approach can also be used in analyzing the thermoelastic damping in out-of-plane vibration of circular plates.

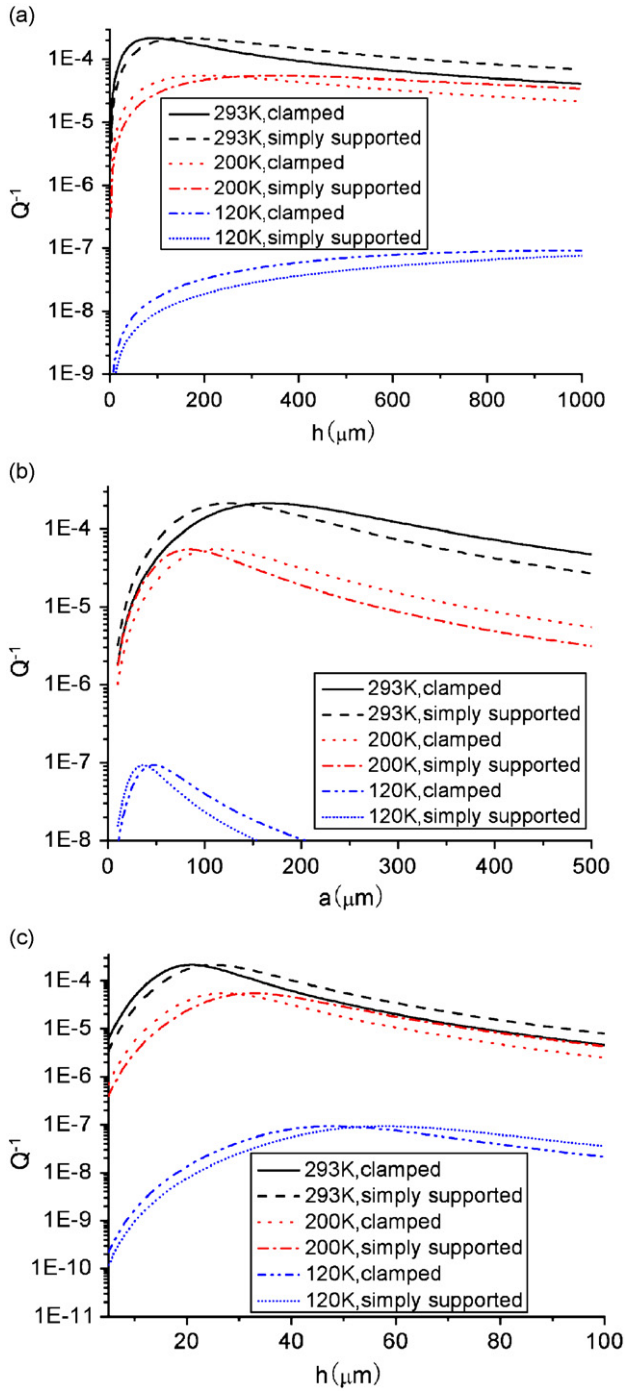

Fig. 3. Thermoelastic damping in silicon circular plate plotted for different geometries under different boundary conditions and environmental temperatures: (a) fixed aspect ratio $a/h = 50$, change h; (b) fixed thickness $h = 10\,\mu\text{m}$, change a and (c) fixed radius $a = 500\,\mu\text{m}$, change h.

5.4. Higher modes of vibration

Fig. 4 illustrates the variation of Q^{-1} with thickness h for circular plates with fixed aspect ratio of $a/h = 50$ under the temperature of $T_0 = 293\,\text{K}$ for modes of $n = 1, 2, 3$. It is known from Section 5.3 that the tendency

Table 2
Critical thickness of plate for $a/h = 50$ and percentage difference based on Zener's approach

T_0 (K)	120	200	293
Clamped plate			
h_c (μm)			
Zener's approach	1099	197.7	89.99
Present method	1102	198.2	90.24
Difference (%)	0.273	0.253	0.278
Simply supported plate			
h_c (μm)			
Zener's approach	1940	349.2	159.0
Present method	1946	350.1	159.4
Difference (%)	0.309	0.258	0.252

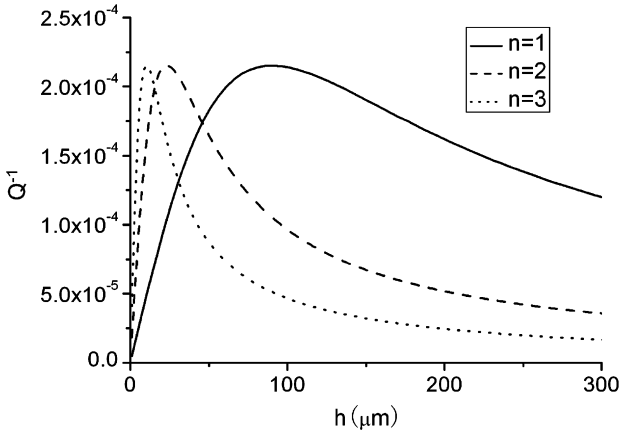

Fig. 4. Variation of Q^{-1} with thickness h for modes of $n = 1, 2, 3$. The aspect ratio is fixed as $a/h = 50$ and the environmental temperature is $T_0 = 293$ K.

of Q^{-1} for simply supported plate is similar to that for clamped plate, so Fig. 4 only shows the case of clamped plate for the purpose of brevity.

It can be seen from Eq. (41) that the frequency with thermoelastic coupling effect being ignored increases with mode number n. In general terms, this might cause a larger or a smaller Q^{-1}, depending on the comparison between ω_0^{-1} and τ_R. However, the maximum value of Q^{-1} maintains the same value for different vibration mode. This also demonstrates that $Q_{\max}^{-1}$ depends on nothing but the temperature.

The curves in Fig. 4 show that the characteristic thickness becomes smaller for higher vibration mode. This can be analyzed through the expression of characteristic thickness. In the present method, the characteristic thickness is obtained through the expression of $\mathrm{d}Q^{-1}/\mathrm{d}h = 0$. However, it is very difficult to get the expression of h_c due to the complexity of the expression of Q^{-1}. Since the percentage difference between the present method and Zener's theory is very small, we can obtain the expression through Zener's theory, i.e., the equation of $\tau_R = \omega_0^{-1}$. According to Eqs. (41) and (47), we can get the following expression of h_c for the circular plate with fixed aspect ratio of $a/h = 50$:

$$h_c = \frac{2500\pi^2\kappa}{q_n\rho c_v}\sqrt{\frac{E}{12(1-\nu^2)}} \tag{48}$$

It is known that q_n shows larger value for higher vibration mode. As a result, h_c gets smaller for higher vibration mode, as shown in Fig. 3.

6. Conclusions

This paper derived the coupling equations for thermoelastic coupling problem in axisymmetric out-of-plane vibration of circular plate and then obtained the exact expression for thermoelastic damping.

It is shown that the thermoelastic damping depends on temperature clearly and it is a significant loss mechanism at room temperature for micro-scale circular plate resonators.

In addition, the thermoelastic damping also changes with the plate dimensions and boundary conditions. There is a critical dimension at which the maximum of thermoelastic damping occurs, and this maximum value is found to be governed by the environmental temperature. On the other hand, in the temperature range of 120–293 K, Q^{-1} increases with the environmental temperature. Finally, it is found that Zener's thermoelastic damping approach can also be used in analyzing the out-of-plane vibration of circular plates.

Acknowledgment

The authors would like to acknowledge Prof. M. Saka for his valuable discussions on this research work. This work was supported by Grant-in-Aid for JSPS Fellow 19 P07097.

References

[1] J.R. Barnes, R.J. Stephenson, M.E. Welland, C.H. Gerber, J.K. Gimzewski, Photothermal spectroscopy with femtojoule sensitivity using a micromechanical device, *Nature* 372 (1994) 79–81.
[2] R.E. Mihailovich, J.M. Parpia, Low temperature mechanical properties of boron-doped silicon, *Physical Review Letters* 68 (1992) 3052–3055.
[3] B. Yurke, D.S. Greywall, A.N. Pargellis, P.A. Busch, Theory of amplifier-noise evasion in an oscillator employing a nonlinear resonator, *Physical Review A* 51 (1995) 4211–4229.
[4] M. Tortonese, R.C. Barrett, C.F. Quate, Atomic resolution with an atomic force microscope using piezoresistive detection, *Applied Physics Letters* 62 (1993) 834–836.
[5] D. Zook, W. Burns, R. Herb, H. Guckel, W. Kang, Y. Ahn, Optically excited self-resonant microbeams, *Sensors and Actuators A* 52 (1996) 92–98.
[6] A.N. Cleland, M.L. Roukes, Fabrication of high frequency nanometer scale mechanical resonators from bulk Si crystals, *Applied Physics Letters* 69 (1996) 2653–2655.
[7] R. Lifshitz, M.L. Roukes, Thermoelastic damping in micro- and nanomechanical systems, *Physical Review B* 61 (2000) 5600–5609.
[8] A.I. Akhiezer, V.B. Berestetskii, *Quantum Electrodynamics*, Interscience Publishers, New York, 1965.
[9] R.E. Mihailovich, N.C. MacDonald, Dissipation measurements of vacuum-operated single-crystal silicon microresonators, *Sensors and Actuators A* 50 (1995) 199–207.
[10] C.L. Zhang, G.S. Xu, Q. Jiang, Analysis of the air-damping effect on a micromachined beam resonator, *Mathematics and Mechanics of Solids* 8 (2003) 315–325.
[11] D.A. Harrington, P. Mohanty, M.L. Roukes, Energy dissipation in suspended micromechanical resonators at low temperatures, *Physica B* 284–288 (2000) 2145–2146.
[12] Y.X. Sun, D.N. Fang, A.K. Soh, Thermoelastic damping in micro-beam resonators, *International Journal of Solids and Structures* 43 (2006) 3213–3229.
[13] H. Hosaka, K. Itao, K. Kuroda, Damping characteristics of beam-shaped micro-oscillators, *Sensors and Actuators A* 49 (1995) 87–95.
[14] D.W. Carr, L. Sekaric, H.G. Craighead, Measurement of nanomechanical resonant structures in single-crystal silicon, *Journal of Vacuum Science and Technology B* 16 (1998) 3821–3824.
[15] D.N. Fang, Y.X. Sun, A.K. Soh, Advances in thermoelastic damping in micro- and nano-mechanical resonators: a review, *Journal of Solid Mechanics and Materials Engineering* 1 (2007) 18–34.
[16] C. Zener, Internal friction in solids I. Theory of internal friction in reeds, *Physical Review* 52 (1937) 230–235.
[17] C. Zener, Internal friction in solids II. General theory of thermoelastic internal friction, *Physical Review* 53 (1938) 90–99.
[18] C. Zener, W. Otis, R. Nuckolls, Internal friction in solids III. Experimental demonstration of thermoelastic internal friction, *Physical Review* 53 (1938) 100–101.
[19] B.S. Berry, Precise investigation of the theory of damping by transverse thermal currents, *Journal of Applied Physics* 26 (1955) 1221–1224.
[20] R.V. Roszhardt, The effect of thermoelastic internal friction on the Q of micromachined silicon resonators, *IEEE Solid State Sensor and Actuator Workshop*, Hilton Head Island, SC, USA, 1990, pp. 13–16.
[21] K.Y. Yasumura, T.D. Stowe, T.W. Kenny, D. Rugar, Thermoelastic energy dissipation in silicon nitride microcantilever structures, *Bulletin of the American Physical Society* 44 (1999) 540.
[22] B.H. Houston, D.M. Photiadis, J.F. Vignola, M.H. Marcus, X. Liu, D. Czaplewski, L. Sekaric, J. Butler, P. Pehrsson, J.A. Bucaro, Loss due to transverse thermoelastic currents in microscale resonators, *Materials Science and Engineering A* 370 (2004) 407–411.

[23] V.T. Srikar, S.D. Senturia, Thermoelastic damping in fine-grained polysilicon flexural beam resonators, *IEEE Journal of Microelectromechanical Systems* 11 (2002) 499–504.
[24] G. Bao, W. Jiang, A heat transfer analysis for quartz microresonator IR sensors, *International Journal of Solids and Structures* 35 (1998) 3635–3653.
[25] J.R. Vig, R.L. Filler, Y. Kim, Uncooled IR imaging array based on quartz resonators, *IEEE Journal of Microelectromechanical Systems* 5 (1996) 131–137.
[26] H. Ziegler, J. Tiesmeyer, Digital sensor for IR radiation, *Sensors and Actuators A* 4 (1983) 363–367.
[27] M.R. Hamrour, S. Galliou, Analysis of the infrared sensitivity of a quartz resonator application as a thermal sensor, *Proceedings of the Ultrasonic Symposium*, Vol. 36, Cannes, France, 1994, pp. 513–516.
[28] S.J. Wong, C.H.J. Fox, S. McWilliam, Thermoelastic damping of the in-plane vibration of thin silicon rings, *Journal of Sound and Vibration* 293 (2006) 266–285.
[29] C.H. Huang, Transverse vibration analysis and measurement for the piezoceramic annular plate with different boundary conditions, *Journal of Sound and Vibration* 283 (2005) 665–683.
[30] The Institution of Electrical Engineers, *Properties of Silicon*, INSPEC, London, New York, 1988.
[31] U. Gysin, S. Rast, E. Meyer, D.W. Lee, P. Vettiger, C. Gerber, Temperature dependence of the force sensitivity of silicon cantilevers, *Physical Review B* 69 (2004) 045403.